

A Note on Saturation Seen in the MDI/SOHO Magnetograms

Y. Liu · A.A. Norton · P.H. Scherrer

Received: 22 August 2006 / Accepted: 14 January 2007 /
Published online: 14 March 2007
© Springer 2007

Abstract A type of saturation is sometimes seen in sunspot umbrae in MDI/SOHO magnetograms. In this paper, we present the underlying cause of such saturation. By using a set of MDI circular polarization filtergrams taken during an MDI line profile campaign observation, we derive the MDI magnetograms using two different approaches: the *on-board data processing* and the *ground data processing*, respectively. The algorithms for processing the data are the same, but the former is limited by a 15-bit lookup table. Saturation is clearly seen in the magnetogram from the *on-board processing* simulation, which is comparable to an observed MDI magnetogram taken one and a half hours before the campaign data. We analyze the saturated pixels and examine the on-board numerical calculation method. We conclude that very low intensity in sunspot umbrae leads to a very low depth of the spectral line that becomes problematic when limited to the 15-bit on-board numerical treatment. This 15-bit on-board treatment of the values is the reason for the saturation seen in sunspot umbrae in the MDI magnetogram. Although it is possible for a different type of saturation to occur when the combination of a strong magnetic field and high velocity moves the spectral line out of the effective sampling range, this saturation is not observed.

1. Introduction

The primary observable of the MDI/SOHO, the Doppler velocity, is derived from four filtergrams, $F1-4$, taken at four wavelengths equally spaced by 75 m\AA across the Ni I spectral line at 6768 \AA (Scherrer *et al.*, 1995). These four filtergrams are used to compute a ratio of differences of the intensities, α , and this ratio is then calibrated by an on-board lookup table

Y. Liu (✉) · P.H. Scherrer
W.W. Hansen Experimental Physics Laboratory, Stanford University, Stanford,
CA 94305-4085, USA
e-mail: yliu@quake.stanford.edu

A.A. Norton
National Solar Observatory, 950 N. Cherry Ave., Tucson, AZ 85719, USA

to become a Doppler velocity. The ratio α is defined as:

$$\begin{aligned} \alpha &= (sa + sc)/sa && \text{if } sa + sc > 0, \quad \text{or,} \\ \alpha &= (sa + sc)/(-sc) && \text{if } sa + sc \leq 0, \end{aligned} \quad (1)$$

where $sa = F1 - F3$ and $sc = F2 - F4$ (see Scherrer *et al.*, 1995 for more detail). A line-of-sight magnetogram is determined using the difference of two Dopplergrams from left and right circular polarization. Sometimes saturation is seen in sunspot umbrae in the magnetograms.

Generally, the “classic” magnetograph saturation occurs when the magnetic field is very strong (see, *e.g.* Svalgaard, Duvall, and Scherrer, 1978; Ulrich *et al.*, 2002 for more detail). This is because the lobes of the Stokes V profile stop growing in amplitude and start to separate. The traditional magnetograph formula is not appropriate to use in the strong field regime due to its insensitivity to increasingly strong fields once the Stokes V lobes begin to separate. However, MDI does not use the traditional magnetograph formula but instead uses a modified center of gravity method (see Landi Degl’Innocenti, 1992 for a good review) that does not suffer from the “classic” saturation effects (see Rees and Semel, 1979).

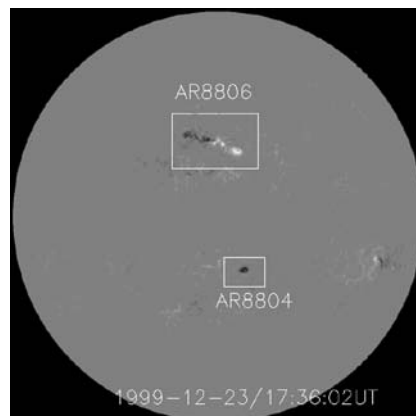
A combination of high velocity and strong magnetic fields can cause some filter-type magnetographs to saturate for a different reason. Namely, the spectral line of a magnetograph is shifted by a wavelength displacement due to the Zeeman effect and Doppler shifting away from the sampling wavelengths.

In this research, we present a detailed analysis to understand specifically what causes the saturation seen in the MDI magnetograms. The paper is organized as follows. A typical saturation in the MDI magnetograms is exhibited in Section 2. In Section 3, we simulate MDI measurements of magnetic field from modeled spectral line profiles and also from the observed data taken from an MDI line profile campaign observation. An analysis is presented in Section 4 and our conclusions are found in Section 5.

2. Saturation Seen in MDI Magnetograms

We present in Figure 1 a typical saturation phenomenon in an MDI full disk magnetogram. The figure exhibits two active regions, AR8806 in the northern hemisphere and AR8804 in the southern hemisphere. Both active regions are near the disk center and both demonstrate

Figure 1 Full disk line-of-sight magnetogram taken by MDI/SOHO at 17:36UT of December 23, 1999. There were two active regions, AR8806 and AR8804, near the disk center in the opposite hemispheres. Both show saturation in the leading polarity sunspots.



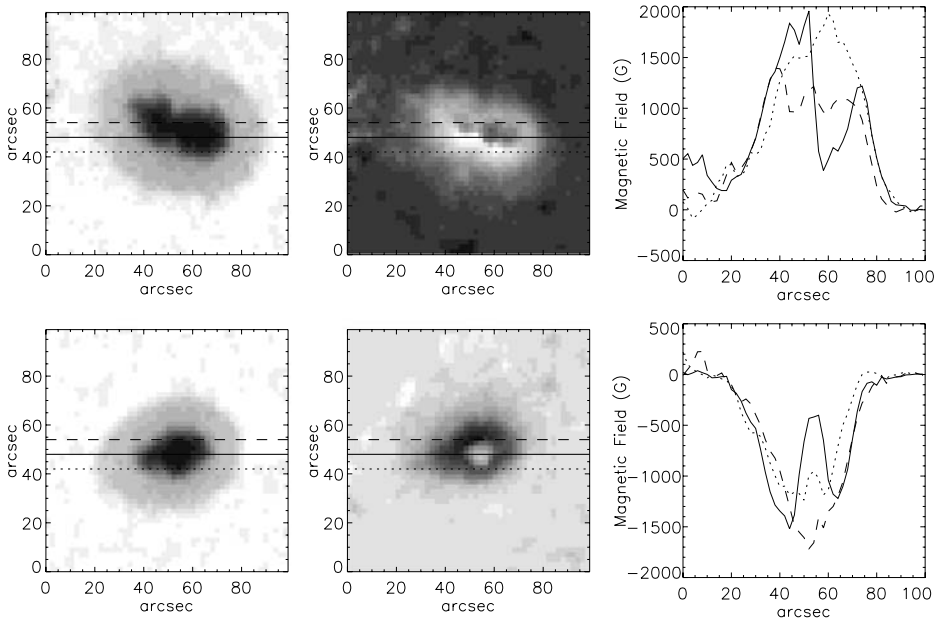


Figure 2 Intensity images (left panels), magnetograms (middle) and line of sight magnetic field strengths along the lines shown in the middle panels (right), for AR8804 (bottom panels) and AR8806 (top panels). The data were taken at 17:35:32 (intensity data) and 17:36:02 (magnetogram) of December 23, 1999 when both regions were near the solar disk center. It is seen that the saturation occurred in the umbrae (the solid lines).

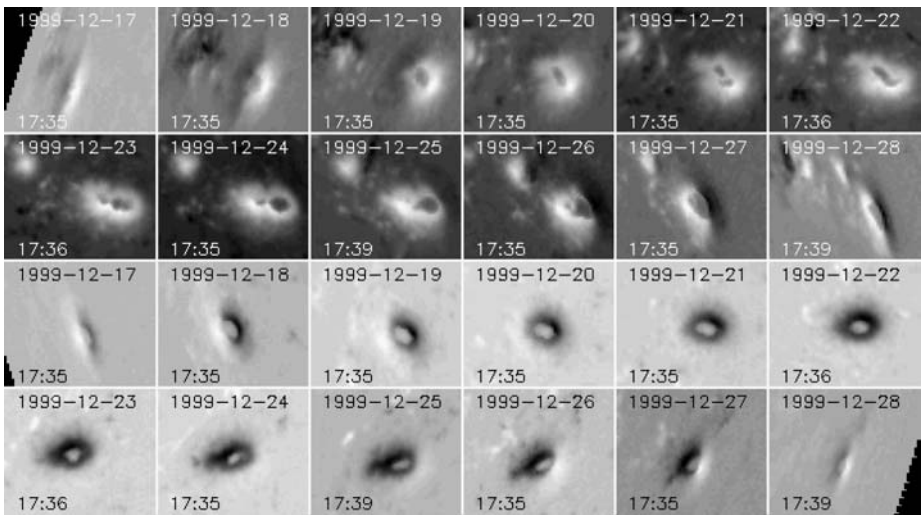
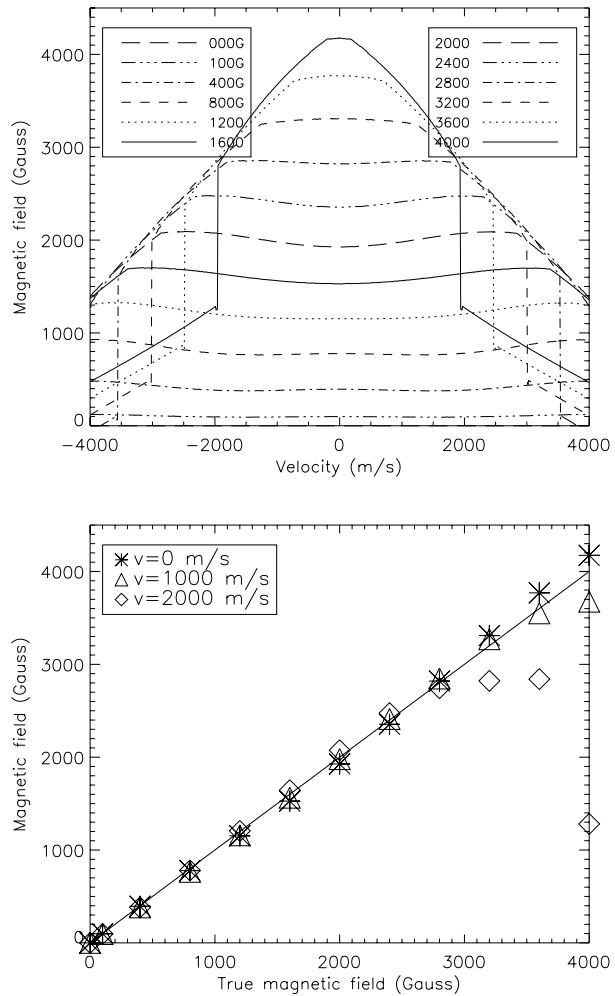


Figure 3 Time-series magnetogram snapshots showing disk passage of both active regions. The top two panels exhibit magnetic field of the leading sunspot of AR8806 from December 17 to 28, while the bottom two panels present magnetic field of AR8804 for the same time interval. The saturation persists for the entire disk passage of both regions.

Figure 4 Simulation of the magnetic field measurements from MDI. The line profile is computed from a sunspot umbral model (Maltby *et al.*, 1986; model M). The inclination angle of magnetic field is set to be zero and the location is at the disk center. Top: MDI measured magnetic field versus velocity. The different lines represent different true magnetic fields. Bottom: MDI measured field versus true magnetic field. The solid line illustrates measurement = true magnetic field. The symbols represent different velocities.



saturation in the leading polarity. The saturation occurs in the sunspot umbrae (see Figure 2) and persists for the entire disk passage of the active regions (see Figure 3). Therefore, the MDI saturation is not a phenomenon dependent upon viewing angle or background velocity.

3. Simulation

3.1. Simulation of MDI Measurement from Modeled Line Profiles

We simulate an MDI observation to study this saturation problem. This simulation includes the MDI optical system, the MDI algorithms for computing the observables, and the on-board data processing. The Stokes parameter profiles of Ni I 6768 Å are calculated based on a sunspot umbral model proposed by Maltby *et al.* (1986). We use the umbral M model that is an average umbral core model. The simulation shows that saturation due to the spectral line moving outside the sampling range can only occur for strong magnetic field with fairly

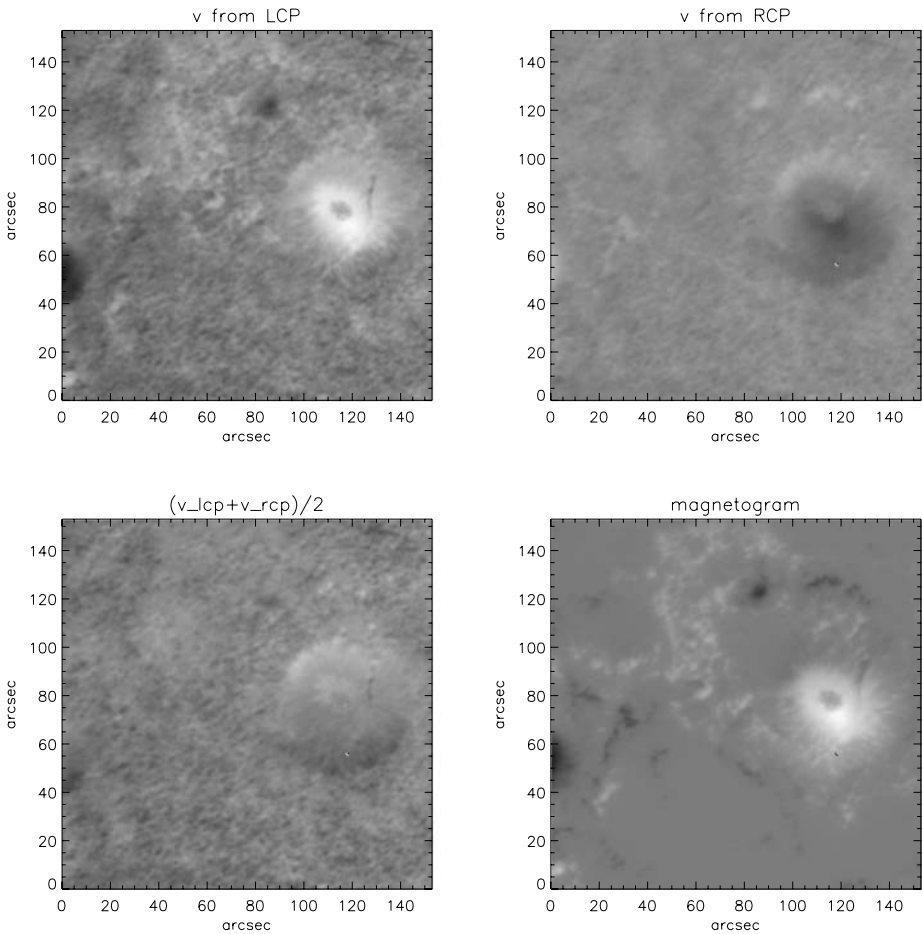


Figure 5 Dopplergrams and magnetograms from an MDI line profile campaign data computed from the on-board mode simulation. The top panels show Dopplergrams from left circular polarization (left) and right circular polarization (right) observation, while the bottom panels show average of these two Dopplergrams (left), and the magnetogram (right). See text for more detail.

high velocity. For example, measurements become saturated for an umbral field strength of 2800 gauss when the velocity is $\pm 2000 \text{ m s}^{-1}$, roughly the rotational velocities at the limb (see Figure 4).

MDI measurements have not been observed to saturate simply due to velocities alone. The highest velocities observed on the disk, those in granular lanes and those due to rotation, are simply not strong enough to move non-magnetic line profiles outside the filter sampling range. Considering that saturation persists for the entire disk passage of the active regions (see Figure 3), it is not possible that the profiles are simply being shifted outside the filter sampling range.

3.2. Simulation of MDI Measurement from Observational Line Profiles

A simulation of the MDI measurement was performed using observational line profile data. The data were taken at 09:46 UT on May 20, 2000 in high resolution during a line profile

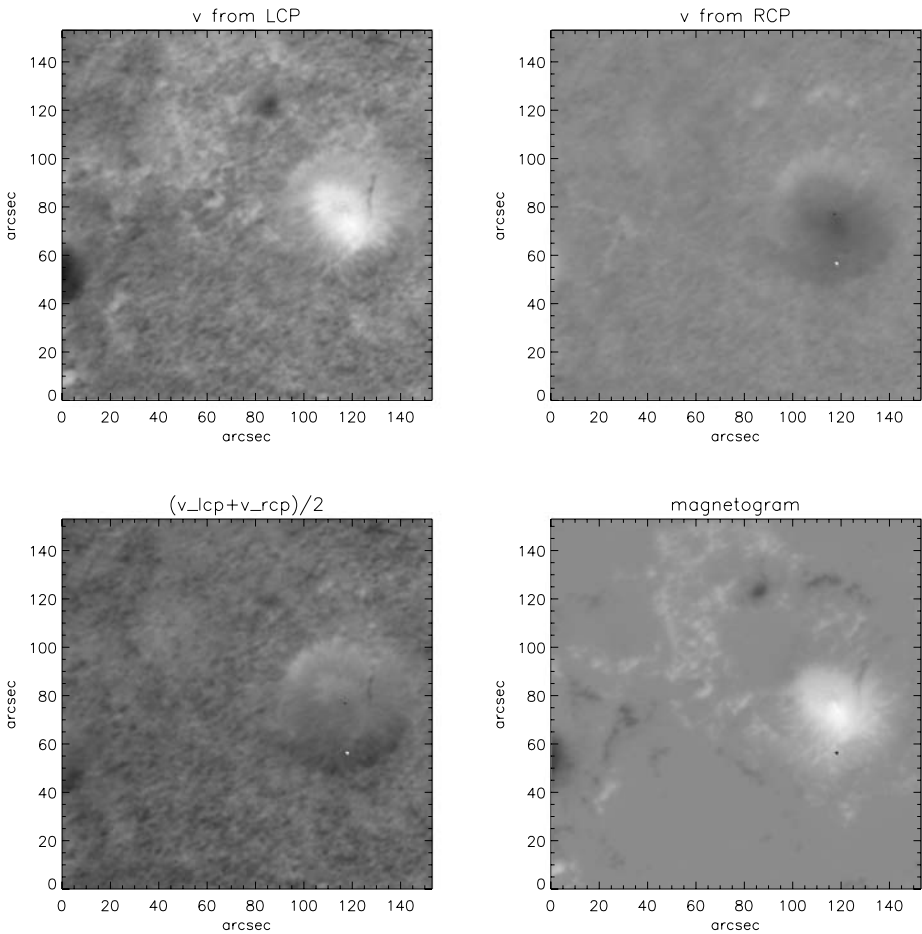
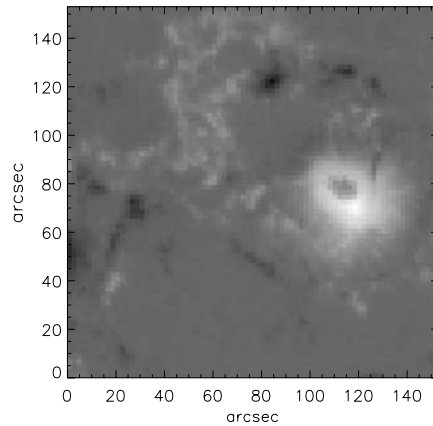


Figure 6 Same as in Figure 5, but computed from the ground mode simulation.

campaign observation. In this observation, the circular polarization filtergrams at the four wavelengths were taken and down-linked to the ground without on-board data processing. The observational area was near the disk center and included an active region, AR9002. We simulate the MDI measurement in two ways: (1) the data are processed using the on-board mode, which allows only a 15-bit computation; and (2) the data are processed using a more accurate calculation (referred to as ground mode hereafter). The algorithms are the same, employing the MDI algorithm used for computing the observables, excepting that the on-board algorithm employs a 15-bit data processing with a lookup table.

Figure 5 shows the results from the on-board mode. From top to bottom and left to right are the velocity fields from left circular polarization and right circulation, the average of these two fields, and the magnetic field. The saturation is seen clearly in the sunspot umbra. In contrast, in the ground mode results shown in Figure 6, the distinctive saturation signature is not present. Figure 7 shows a routine MDI magnetogram image of this active region taken one and a half hours before the campaign data. The image compares favorably to Figure 5 and suggests that the on-board data processing is causing the saturation.

Figure 7 Magnetogram as observed in MDI full disk mode taken one and half hours before the line profile campaign data. This is the routine observable as calculated using on-board calibration. The saturation is clearly seen in the sunspot umbra. Note that campaign data shown in Figures 5 and 6 were taken in MDI high resolution mode, hence the difference in image quality.



4. Analysis

We present in Figure 8 a more detailed analysis of this saturation. Plotted in the upper left panel is a sub-image of the magnetogram computed by the on-board mode (see also Figure 5). The pixels we analyze are on the thick black line crossing the saturation area. Two vertical lines identify the saturation pixels. The magnetic fields of those pixels computed from on-board mode and ground mode are exhibited in solid and dashed lines in the upper right panel. It is not surprising that the fields are the same except the saturation pixels: it is apparent that the on-board mode results in saturated values, while the values from the ground mode look more or less constant. The ground mode may also be somewhat problematic for those pixels as the signal becomes noisy. The bottom left panel shows the intensities $F2-4$ are almost identical in the saturated pixels but intensity $F1$ is brighter: it probably implies that the line depth is very small while part of $F1$ bandpass has shifted away from the line profile due to strong magnetic field.

The reason that the saturation from the on-board mode simulation is much more striking than that from the ground mode simulation is that the on-board data processing uses a 15-bit lookup table for the α computation (see (1)) that is now proven to be too small. More specifically, this intensity ratio is proportional to $3 \times 2^{20}/(\text{denominator})$, where the denominator is either sa or sc . When it is less than $3 \times 2^5 (= 96)$ the saturation level of 2^{15} is exceeded. Such numerical limitation is certainly avoided when a floating computation is allowed. This is why we don't see a similar saturation in the ground mode simulation (see Figure 6). It is not surprising that sa and sc of the saturation pixels have values below 96 (see the bottom right panel of Figure 8). We extended such an analysis to the whole image. As expected, the denominator in all the saturated pixels falls below 96.

The low intensity coupled with the MDI 15-bit on-board algorithm is the cause of the saturation seen in MDI magnetograms. It is well-known that within sunspot umbrae there is a locally defined intensity–magnetic field ($I-B$) relationship in which the intensity becomes lower as the magnetic field becomes stronger (see Martinez Pillet and Vasquez, 1993). Such low intensity leads to a shallow line profile. This profile is further contaminated by molecular lines that become more prominent in the coolest regions of sunspot umbrae, and is also contaminated by the noise that may become comparable to the signals when the intensity

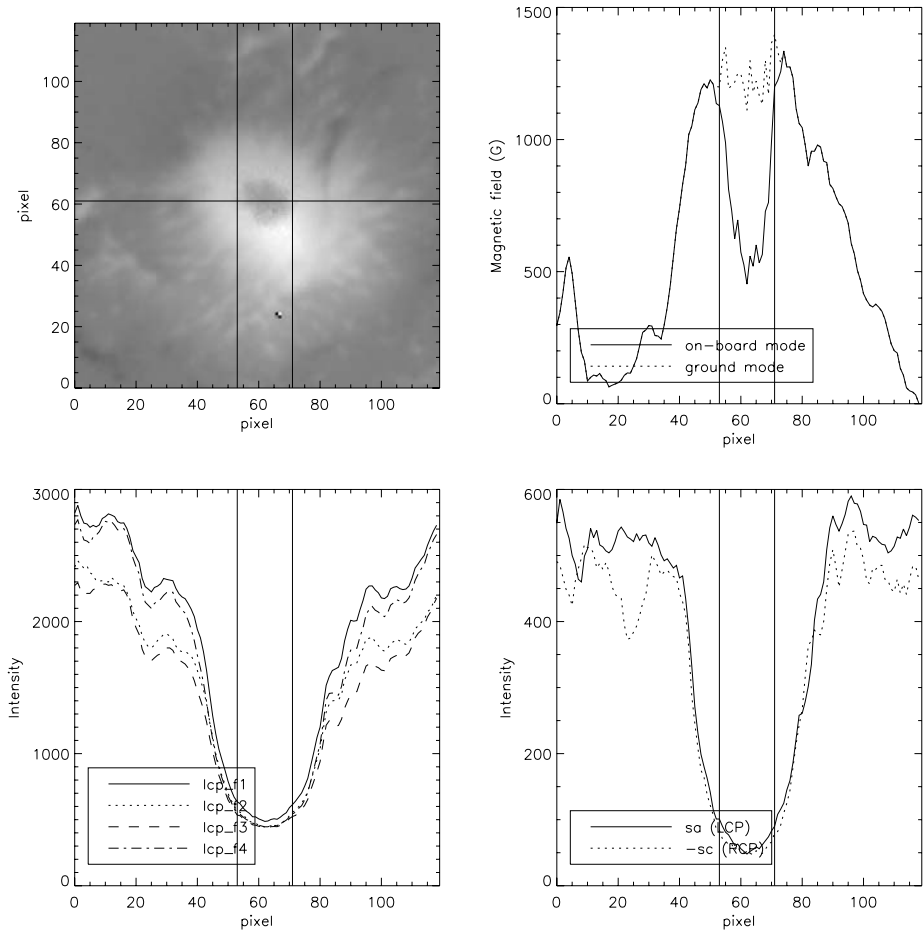


Figure 8 Top left: Part of the magnetogram computed by the on-board mode, as shown in Figure 5. The thick dark line denotes the pixels we analyze in the other three panels. The vertical lines define the saturation pixels. Top right: magnetic fields of the chosen pixels from on-board mode (the solid line) and ground mode (the dashed line) simulations. Bottom left: Intensities of the left circular polarization at four wavelengths, $F1-4$. Bottom right: the differences of intensities of the left circular polarization ($sa = F1 - F3$; solid line) and the right circular polarization ($c = F2 - F4$; dashed line).

is low (but the photon noise is still much below the signal¹). A combination of the above effects causes this spectral line profile to be very shallow and complex (see the left bottom panel of Figure 8). Actually, such a line profile also causes the ground mode calibration to be problematic (see the right top panel of Figure 8). More extensive modeling of the NiII 6768 line formation in the umbrae as observed with the MDI algorithm could have prevented this problem.

¹Considering that the camera system gain is $110 \text{ e}^-/\text{DN}$ (Scherrer *et al.*, 1995), we can estimate the photon noise to be about 2 DN for a 400 DN intensity that is a minimum value in the saturation area, while the signal is still about 50 DN (see the bottom panels of Figure 8).

Approximately 5.2% of active regions (42 out of 814 active regions) observed from March 1999 to December 2000 with MDI showed saturation in their umbrae. Among 42 active regions whose umbrae showed saturation, 86% (36 regions) experienced saturation when they were near disk center. These statistics compare favorably to a recent study of the strongest umbral magnetic fields by Livingston *et al.* (2006) that show 4.6% of spot groups contain a strong field equal to or greater than 3000 gauss.

5. Conclusions

We have researched the saturation phenomenon experienced by MDI when observing sunspot umbrae. The saturation is visible during the entire disk passage of the sunspots. We simulated MDI measurements of line-of-sight magnetic fields based on modeled spectral line profiles as well as analyzing observed line profiles from an MDI line profile campaign. We conclude that the low intensity in the umbrae of sunspots that leads to very small line depth combined with a 15-bit on-board numerical calculation is the major reason causing the saturation. In essence, the 15-bit on-board calculation does not allow for such a small value to be used effectively in the MDI algorithm.

We conclude that caution must be used when analyzing Dopplergram or magnetogram data from strong, dark umbrae as observed by MDI. Note that intensity data from MDI is not affected by this numerical limitation of the on-board algorithm, and as such using the intensity — magnetic field relationship may be a better way to ascertain magnetic field strength data in dark umbrae from MDI data (see Norton and Gilman, 2004). Future missions that choose to use on-board calculations could benefit from recently developed data handling techniques such as the 15-bit pipelined floating point treatment described in Thompson and Wooley (2001).

Acknowledgements We wish to thank R. Bush and A. Kosovichev for valuable discussions and comments. The comments and suggestions from the anonymous referee are appreciated that help improve the manuscript. This work was supported by the NASA NAG5-13261. SOHO is a project of international cooperation between ESA and NASA.

References

- Landi Degl'Innocenti, E.: 1992, In: Sanchez, F., Collados, M., Vazquez, M. (eds.) *Solar Observations: Techniques and Interpretation*, Cambridge University Press, Cambridge, p. 71.
- Livingston, W., Harvey, J.W., Malanuschenko, O.V., Webster, L.: 2006, *Solar Phys.* **239**, 41.
- Maltby, P., Avrett, E.H., Carlsson, M., Kjeldseth-Moe, O., Kurucz, R.L., Loeser, R.: 1986, *Astrophys. J.* **306**, 284.
- Martinez Pillet, V., Vasquez, M.: 1993, *Astron. Astrophys.* **270**, 494.
- Norton, A.A., Gilman, P.: 2004, *Astrophys. J.* **603**, 348.
- Rees, D.E., Semel, M.D.: 1979, *Astron. Astrophys.* **74**, 1.
- Scherrer, P.H., Bogart, R.S., Bush, R.I., Hoeksema, J.T., Kosovichev, A.G., Schou, J., Rosenberg, W., Springer, L., Tarbell, T.D., Title, A., Wolfson, C.J., Zayer, I., MDI Engineering Team: 1995, *Solar Phys.* **162**, 129.
- Svalgaard, L., Duvall, T.L., Jr., Scherrer, P.H.: 1978, *Solar Phys.* **58**, 225.
- Thompson, D.U., Wooley, B.A.: 2001, *IEEE J. Solid-State Circuits* **36**, 299.
- Ulrich, R.K., Evans, S., Boyden, J.E., Webster, L.: 2002, *Astrophys. J. Suppl.* **139**, 259.